J. Phys. B: At. Mol. Opt. Phys. **44** (2011) 175205 (7pp) doi:10.1088/0953-4075/44/17/175205

Fully differential cross sections for the single ionization of He by C^{6+} ions

J Colgan[1], M S Pindzola[2], F Robicheaux[2] and M F Ciappina[3]

[1] Theoretical Division, Los Alamos National Laboratory, NM 87545, USA
[2] Department of Physics, Auburn University, Auburn, AL 36849, USA
[3] ICFO—Institut de Ciences Fotoniques, 08860 Castelldefels (Barcelona), Spain

Received 31 May 2011, in final form 8 July 2011
Published 18 August 2011
Online at stacks.iop.org/JPhysB/44/175205

Abstract
We present fully differential cross sections for the single ionization of He by C^{6+} ions. A time-dependent close-coupling approach is used to describe the two-electron wavefunction in the field of the projectile for a range of impact parameters, and a Fourier transform approach is used to extract fully differential cross sections for a specific momentum transfer. Our calculations are compared to the measurements of Schulz *et al* (2003 *Nature* **422** 48) and we find very good agreement in the scattering plane and good qualitative agreement in the perpendicular plane. In particular, our calculations in the perpendicular plane find a similar 'double-peak' structure in the angular distributions to those seen experimentally. We also discuss the various checks made on our calculations by comparing to a one-electron time-dependent calculation.

(Some figures in this article are in colour only in the electronic version)

1. Introduction

The single ionization of few-electron atoms by charged-ion impact has been a fruitful field of study for many years [2]. At high impact energies, it had been expected that all measurable quantities from such reactions could be well described by perturbation theory, when the perturbation ($\sim |Z_P|/v_P$) caused by a projectile of charge Z_P and velocity v_P is small. However, measurements made of the fully differential cross sections (FDCS) of single ionization of He by fully stripped carbon ions with a velocity of 100 MeV amu^{-1} [1], where $|Z_P|/v_P \sim 0.1$, found unexpected structure in the perpendicular plane. This plane is perpendicular to the 'scattering' plane defined by the incoming projectile direction (which defines the z-axis) and the direction of the transverse momentum transfer. The structure found in the measurements was not found in first-Born-approximation (FBA) calculations [1, 3], in which the angular distributions were almost flat in this plane, although such calculations and measurements were in good agreement for the angular distributions in the scattering plane. Furthermore, the magnitude of the FBA cross section in the perpendicular plane was considerably smaller than that found experimentally.

This unexpected result generated much discussion and theoretical investigation. Although the structure in the perpendicular plane was attributed to higher-order effects [1], a subsequent theoretical investigation [4] which included the second-Born contribution was not able to reproduce the earlier measurements. In fact, the inclusion of the second Born contribution actually worsened the comparison with experiment, although this may have been influenced by the choice of a rather approximate helium initial state. Later studies also found that an improved treatment of the ejected-electron–ion interactions made little difference to the calculations, and it was demonstrated that the agreement between experiment and theory grew steadily worse as one moved from the scattering to the perpendicular plane [5]. It was then asserted [6] that the perpendicular plane structure in the measurements was largely due to experimental resolution issues caused by the temperature of the target gas, although this explanation was later refuted [7]. An alternative explanation for the perpendicular plane structure was subsequently proposed in terms of elastic scattering of the projectile by the helium nucleus [8], and a more recent study indicated that convoluting the experimental resolution within a calculation may increase the magnitude of the cross section in the perpendicular plane [9]. A very recent calculation, which employed coupled pseudostates within an impact parameter treatment of the projectile interaction [10], again found good agreement with measurement in the scattering plane, but a

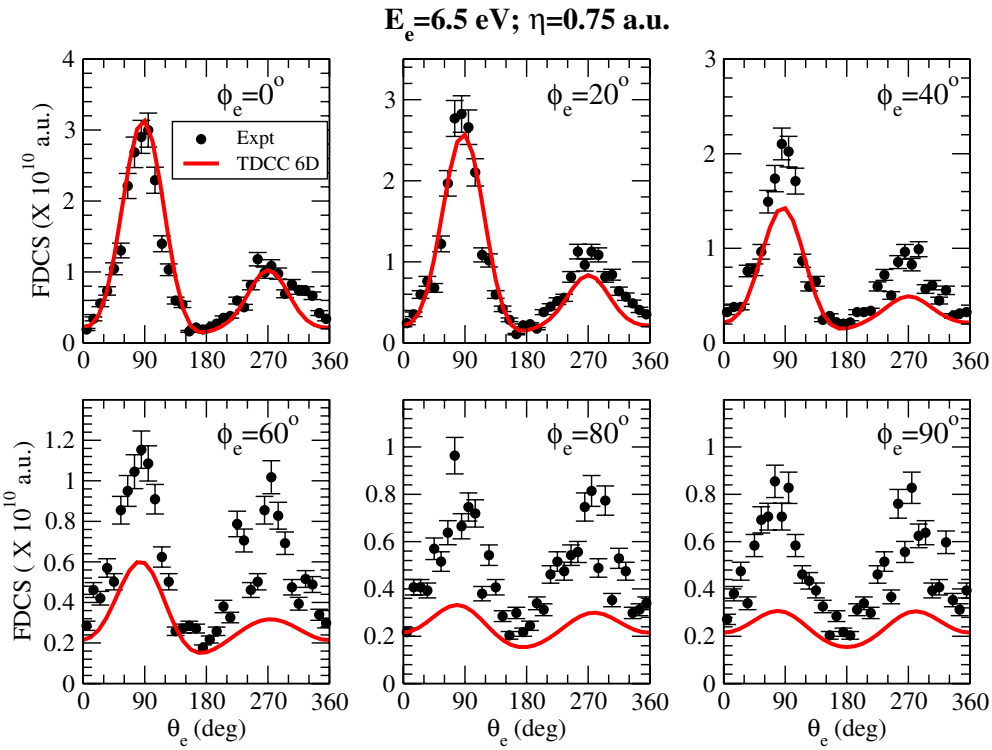

Figure 1. FDCS for single ionization of helium by 100 MeV amu^{-1} C^{6+} ions for various values of the ejected electron azimuthal angle ϕ_e, for a momentum transfer of $\eta = 0.75$ au, and an ejected electron energy $E_e = 6.5$ eV. The measurements of [1] are compared with TDCC two-electron calculations (labelled as TDCC 6D).

flat angular distribution, in conflict with experiment, in the perpendicular plane.

In this paper, we also investigate the single ionization of helium by C^{6+} ion impact at 100 MeV amu^{-1}. We use the time-dependent close-coupling approach (TDCC) [11, 12] to calculate the FDCS for a range of impact parameters, and then employ a Fourier transform technique [13, 14] to extract the FDCS for a specific momentum transfer. Our approach thus builds on our earlier work [12], in which we investigated the form of the FDCS for this process at specific impact parameters, which was in good qualitative agreement with an earlier semi-classical study [15]. Previous TDCC calculations have found good agreement with experiment for the total single and double ionization of helium by α-particle [11] and anti-proton impact [16]. Atomic units are used unless otherwise stated.

2. Theory

We follow our previous work on single and double ionization of helium by fast ion impact [11, 12] and solve the time-dependent Schrödinger equation for one or two active electrons, where the projectile (with mass m_P and velocity v_P) interaction with the electrons is treated via a multipole expansion [11], and where terms up to octopole are included in our expansion. Following the time-dependent propagation to a final time T, one can obtain single-ionization momentum-space wavefunctions for various impact parameters by a suitable projection.

In the one-electron TDCC approach (now referred to as TDCC 3D), the single-ionization momentum-space wavefunction is given by

$$P_{lm}(k, b) = \int \mathrm{d}r\, P_{kl}(r)\, \bar{P}_{lm}(r, b, T), \tag{1}$$

where $P_{kl}(r)$ is a box-normalized continuum function. The wavefunction $\bar{P}_{lm}(r, b, T)$ is obtained by removing the overlap with the initial ground state of helium using

$$\bar{P}_{lm}(r, b, T) = P_{lm}(r, b, t) - \alpha P_{1s}(r)\delta_{l,0}\delta_{m,0}, \tag{2}$$

with

$$\alpha = \int \mathrm{d}r\, P_{1s}(r)\, P_{00}(r, b, T). \tag{3}$$

Here, $P_{1s}(r)$ is a bound radial orbital obtained by diagonalization of the one-electron Hamiltonian given by

$$H(r) = -\frac{1}{2}\frac{\partial^2}{\partial r^2} - \frac{Z_t}{r} + V_l(r), \tag{4}$$

where $Z_t = 2$ for helium, and $V_l(r)$ is a Hartree local exchange potential for the atomic core.

In the two-electron TDCC approach (now referred to as TDCC 6D), the single-ionization momentum-space wavefunction is given by

$$P_{0L}^{LM}(1s, k, b) = \int \mathrm{d}r_1 \int \mathrm{d}r_2\, \bar{P}_{0L}^{LM}(r_1, r_2, b, T)\, P_{1s}(r_1)\, P_{kL}(r_2). \tag{5}$$

The wavefunction $\bar{P}^{LM}_{0L}(r_1, r_2, b, T)$ is obtained by removing the overlap with the initial ground state of helium using

$$\bar{P}^{LM}_{0L}(r_1, r_2, b, T) = P^{LM}_{0L}(r_1, r_2, b, t) - \beta \hat{P}^{00}_{00}(r_1, r_2)\delta_{L,0}\delta_{M,0}, \quad (6)$$

with

$$\beta = \sum_l \int \mathrm{d}r_1 \int \mathrm{d}r_2 \hat{P}^{00}_{ll}(r_1, r_2) P^{00}_{ll}(r_1, r_2, T) \quad (7)$$

and where $\hat{P}^{00}_{ll}(r_1, r_2)$ is the initial ground state of He, obtained by relaxation of the time-dependent Schrödinger equation without electron–projectile coupling terms.

In both the one- and two-electron TDCC formulations, the single-ionization momentum-space wavefunction can be used to construct a function which depends on the angles of the ejected electron, using

$$P(\hat{k}, b) = \sum_{lm} (-\mathrm{i})^l \, \mathrm{e}^{\mathrm{i}(\sigma_l + \delta_l)} P_{lm}(k, b) Y_{lm}(\hat{k}) \quad (8)$$

for the one-electron case, and

$$P(\hat{k}, b) = \sum_{LM} (-\mathrm{i})^L \, \mathrm{e}^{\mathrm{i}\sigma_L} P^{LM}_{0L}(1s, k, b) Y_{LM}(\hat{k}) \quad (9)$$

for the two-electron case. In equations (8) and (9), σ_l is the Coulomb phase and $Y_{lm}(\hat{k})$ is a spherical harmonic. In equation (8), δ_l is a distorted-wave phase which is due to the $V_l(r)$ potential.

Our approach up to now is identical to our previous work [12], in which differential cross sections were presented for single ionization of helium at specific impact parameters. If we now wish to obtain cross sections differential with respect to the momentum transfer (η) of the projectile, we must perform a Fourier transform of the function in equations (8) and (9) [13]. This is equivalent to cross sections differential with respect to the projectile scattering angle θ_P, since $\eta \approx \mu v_P \theta_P$ for small projectile angle scattering, where μ is the reduced mass $\mu = m_P m_t/(m_P + m_t)$ with m_t the mass of the target helium atom. Such a transform was recently discussed in detail for various ion-impact processes [14] and was also recently used in similar calculations to those presented here [10].

The two-dimensional Fourier transform for a transition amplitude $\mathcal{A}(\mathbf{b})$ is given by [13] as

$$\mathcal{R}(\boldsymbol{\eta}) = \frac{1}{2\pi} \int \mathrm{d}\mathbf{b} \, \mathrm{e}^{\mathrm{i}\boldsymbol{\eta}\cdot\mathbf{b}} \mathcal{A}(\mathbf{b}) \, , \quad (10)$$

where the exponent term may be expanded using the Jacobi–Anger expression [17], so that we may now express our single-ionization momentum-space wavefunction as

$$P(\hat{k}, \eta) = \frac{1}{2\pi} \sum_{n=-\infty}^{n=+\infty} \mathrm{i}^n \int_0^{2\pi} \mathrm{d}\phi_b \, \mathrm{e}^{-\mathrm{i}n\phi_b} \times \int b \, \mathrm{d}b P(\hat{k}, b) \, \mathrm{e}^{\mathrm{i}\delta(b)} J_n(\eta b). \quad (11)$$

Here, $J_n(\eta b)$ is the Bessel function of nth order and ϕ_b is the azimuthal angle of the impact parameter vector $\mathbf{b}$. A detailed discussion of the properties of similar transition amplitudes within a continuum distorted-wave (CDW) model has recently been given by Gulyás *et al* [14], where it was noted that many terms are often required in the expansion over n in equation (11) to obtain converged results. In the calculations presented here, we found that inclusion of terms up to $|n| \leqslant 5$ was sufficient to obtain converged FDCS.

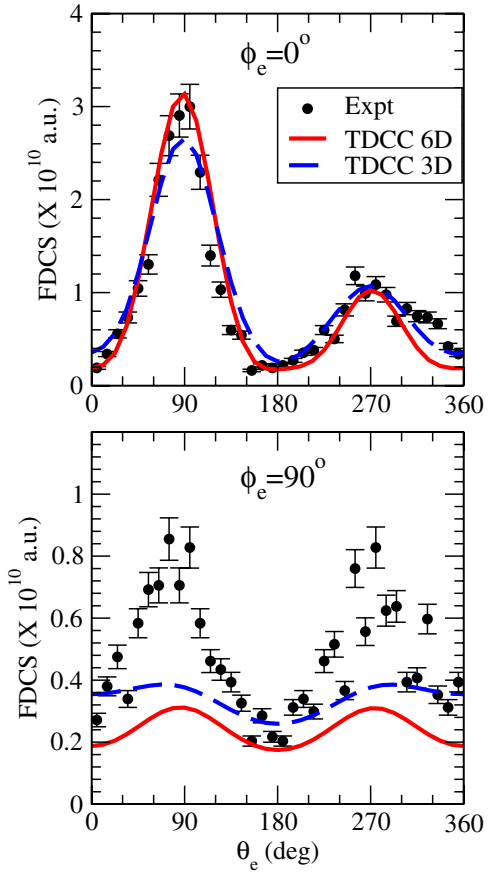

Figure 2. FDCS in the scattering plane (upper panel) and in the perpendicular plane (lower panel) calculated using the TDCC two-electron approach (red solid line, labelled as TDCC 6D) and using the TDCC one-electron approach (blue dashed line, labelled as TDCC 3D). Both sets of calculations are again compared to the measurements of [1].

In equation (11), we have also included a phase factor $\mathrm{e}^{\mathrm{i}\delta(b)}$, which represents the internuclear interaction term. In principle, this term could be included as an extra potential in the TDCC equations, but since this potential is independent of the electron coordinates and is only relevant for cross sections differential in the momentum transfer (or projectile scattering angle), we choose to include this term as a simple phase factor. Following Gulyás *et al* [14], we choose

$$\delta(b) = \frac{2Z_P Z_{\mathrm{eff}}}{v_P} \ln(v_P b), \quad (12)$$

which corresponds to the internuclear interaction potential $V(R) = Z_P Z_{\mathrm{eff}}/R$ with a screened charge $Z_{\mathrm{eff}} = 1.34$. Further discussion of the influence of this factor is given in the following section.

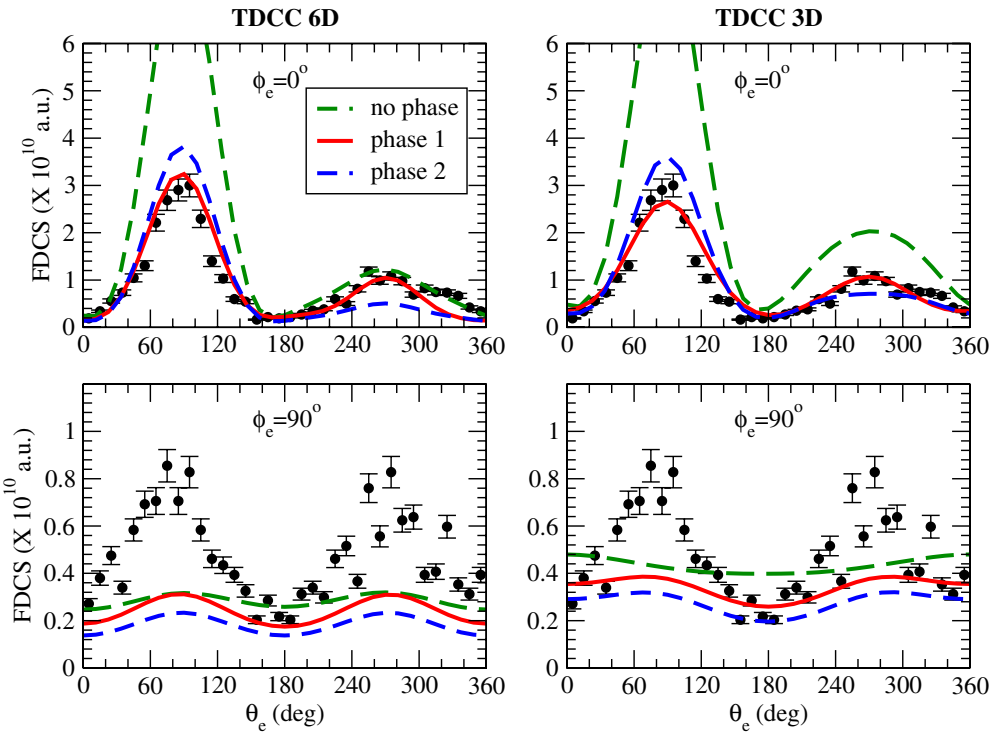

Figure 3. FDCS in the scattering plane (upper panels) and in the perpendicular plane (lower panels). The left panels show two-electron TDCC 6D calculations and the right panels show one-electron TDCC 3D calculations. The red solid lines represent calculations which include the internuclear interaction phase factor $\delta(b)$ in equation (11), and the green dashed lines represent calculations which omit this factor. The blue dashed line indicates calculations using a form of the internuclear interaction phase factor defined by equation (25) of [14].

The FDCS for the single ionization of helium is then given by

$$\frac{\mathrm{d}^4\sigma}{\mathrm{d}\theta_e\,\mathrm{d}\phi_e\,\mathrm{d}k\,\mathrm{d}\eta} = 2|P(\hat{k},\eta)|^2. \tag{13}$$

The pre-factor of 2 is required in the one-electron case as it represents the occupation number of the 1s subshell, and in the two-electron case it arises since we project only onto 1skl product states. We may recover the total single-ionization cross section by integrating over all variables, namely

$$\sigma_{1s} = 2\pi \int \mathrm{d}\eta\,\eta \int \mathrm{d}\phi_e \int \sin\theta_e\,\mathrm{d}\theta_e \int \mathrm{d}k \frac{\mathrm{d}^4\sigma}{\mathrm{d}\theta_e\,\mathrm{d}\phi_e\,\mathrm{d}k\,\mathrm{d}\eta}. \tag{14}$$

Finally, we note that all FDCS presented in this paper are presented in the laboratory frame, where the conversion from the center-of-mass frame (in which the calculations are performed) requires multiplication by a factor of $m_P^2/\mu^2 = 16$ in this case [3].

3. Results and discussion

TDCC calculations for single ionization of helium by C^{6+} impact at 100 MeV amu^{-1} were made using the one- and two-electron formulations as described in the previous section. A radial mesh of 0.1×768 points was used for all radial coordinates, and 300 box-normalized continuum functions, with a spacing of 0.05 au, were used in the projections of equations (1) and (5). In the TDCC 3D calculations, 16 lm channels were used, while 34 coupled $l_1 l_2 LM$ channels were used in the TDCC 6D calculations. The time-dependent equations were propagated from an initial starting point of -50 au (with respect to the target location) to a final distance of over 300 au. In the TDCC 3D calculations, the $P_{1s}(r)$ bound orbital obtained from diagonalization of equation (4) was used as the initial state, and in the TDCC 6D calculations the initial He state was obtained by relaxing the time-dependent equations in imaginary time, without the electron–projectile terms, on the same radial grid, using four ll coupled channels. Calculations were carried out for a range of impact parameters up to $b = 30$ au, with a spacing of $\Delta b = 0.2$ au. FDCS using the Fourier transform approach were found to be insensitive to this spacing being halved. The cross sections presented here did not change noticeably when the range of impact parameters was increased, and our calculations were also found to be well converged with respect to the number of points included in the integral over ϕ_b in equation (11).

In figure 1, we present results from our TDCC 6D calculations, including the Fourier transform, for single ionization of helium by 100 MeV amu^{-1} C^{6+} ions. Calculations made at a momentum transfer of $\eta = 0.75$ au and an ejected electron energy of 6.5 eV are compared to the measurements of Schulz *et al* [1] for various ejected electron azimuthal angles ϕ_e. We note that $\phi_e = 0^\circ$ corresponds to the scattering plane and $\phi_e = 90^\circ$ corresponds to the perpendicular plane. Turning first to the scattering plane calculations ($\phi_e = 0^\circ$), we find excellent agreement between

the calculations and the measurement. The binary and recoil peaks that constitute the cross section are well reproduced in both shape and magnitude. The good agreement for the recoil peak is noteworthy as previous calculations [5, 10] have slightly underestimated this peak.

As the ϕ_e angle is increased towards 90°, we find that in the calculations, the magnitude of the binary peak quickly decreases, and the magnitude of the recoil peak slowly decreases, so that by $\phi_e = 90°$, the cross section is symmetric about $\theta_e = 180°$, as required. More importantly, the perpendicular plane calculations display a double-peak structure, quite similar to that found in the measurements. This is particularly noteworthy, since many sets of previous calculations [4, 5, 10] have found a flat distribution in the perpendicular plane, similar to that found in FBA calculations. The structure in the perpendicular plane found experimentally, and now in our calculations, has long been taken to indicate the importance of higher-order contributions to the scattering amplitude, and was also previously found in our earlier calculations at specific impact parameters [12]. As the ϕ_e angle is increased from 0°, the magnitude of the measurements also decreases, although not as quickly as in the calculations, so that, by $\phi_e = 90°$, there is a considerable magnitude discrepancy between our calculations and the measurements. However, we again emphasize that the shape of the calculated cross section in the perpendicular plane is quite similar to that found experimentally.

In figure 2, we compare our TDCC 3D and TDCC 6D calculations with each other and with the measurements of [1], for the scattering and perpendicular plane cases. The two TDCC approaches are in good agreement with each other in the scattering plane. In the perpendicular plane, the two calculations are in reasonable shape agreement, but differ somewhat in magnitude. The TDCC 6D calculations find a somewhat stronger double-peak structure than the TDCC 3D calculations.

It is hard to determine the reason for the difference in magnitude of the TDCC one-electron and two-electron cross sections, although we do note that the total single-ionization cross sections from the one-electron TDCC calculations are only slightly larger than the total cross section from the two-electron TDCC calculations. At this point, it is also worth noting that the two-electron TDCC calculation can also include the probability for single ionization leaving the He^+ ion in an excited state (for example, 2s or 2p), by similar projection methods to those given by equation (1). However, the contribution to the FDCS from ionization leaving the ion in an excited state was found to be negligible. The most instructive point from figure 2 may be that a TDCC 3D calculation with only one active electron still finds a weak double-peak structure in the perpendicular plane cross section. This effectively rules out any two-electron interaction as the sole reason for this structure.

We now turn to an examination of the influence of the internuclear interaction on the FDCS. Figure 3 shows TDCC calculations again made for the specific case of $\eta = 0.75$ au and E_e = 6.5 eV, where the left panels present TDCC 6D calculations and the right panels present TDCC 3D

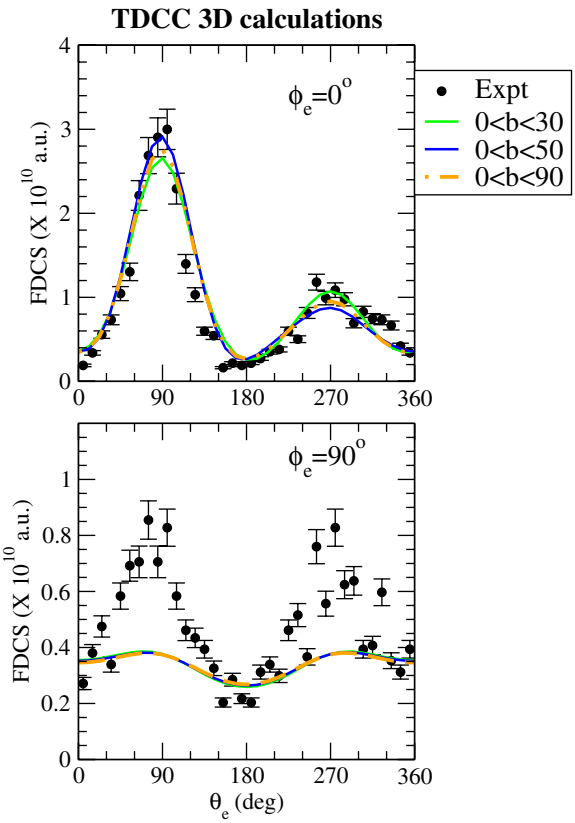

Figure 4. TDCC 3D calculations of the FDCS in the scattering plane (upper panel) and in the perpendicular plane (lower panel). Calculations are presented in which the range of impact parameters used was varied, up to 30 au (solid green line), up to 50 au (solid blue line) and up to 90 au (dashed orange line).

calculations. The green dashed line indicates calculations where the internuclear interaction phase $\delta(b)$ in equation (11) is set to zero. The cross sections in the scattering plane with this choice are in worse agreement with experiment for both sets of TDCC calculations, as the ratio of the binary to recoil peak height is much larger than in the measurement. In the perpendicular plane, the double-peak structure is diminished in the TDCC 6D calculations without the phase factor, and vanishes in the TDCC 3D calculations, where the distribution is almost flat. We thus find that inclusion of the internuclear interaction phase factor is an important component of the FDCS for these cases. Varying the form of the internuclear interaction phase factor in equation (11) (for example, the authors of [14] give an alternative form for the internuclear interaction phase) can slightly change the magnitude of the FDCS, but the characteristic shapes in both the scattering and perpendicular plane, as demonstrated by the solid red lines in figure 3, remain the same. Also, using the full target charge (i.e. $Z_{\rm eff} = 2.0$) in equation (12) gives similar results to calculations presented in figure 3.

Finally, in figure 4 we present TDCC 3D calculations, again for the scattering and perpendicular planes, where we vary the range of impact parameters used in the FDCS calculations. We find that increasing the impact parameter range beyond 30 au (which was the maximum impact parameter used in the calculations presented earlier) makes

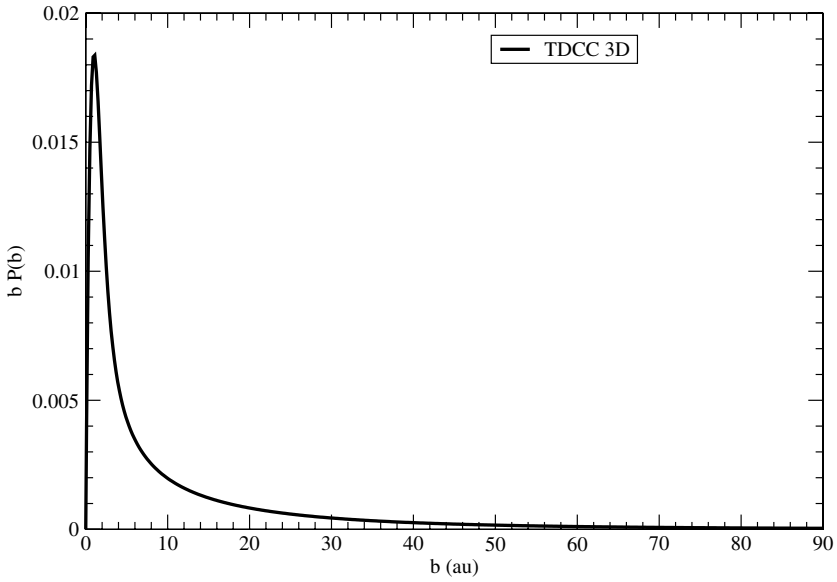

Figure 5. TDCC 3D calculations of the weighted ionization probability for single ionization of helium by 100 MeV amu^{-1} C^{6+} ions, as a function of the impact parameter.

very little difference to the FDCS. This is not surprising, as by 30 au, the single-ionization probability has dropped significantly, as shown in figure 5, and is almost two orders of magnitude lower than at the peak of the probability distribution, which occurs near $b = 1.0$ au. Furthermore, very large impact parameters correspond to very small momentum transfers [12], so we do not expect large impact parameters to contribute to the FDCS at the current momentum transfer value of 0.75 au.

4. Conclusion

We have presented TDCC one-electron and two-electron calculations for the single ionization of helium by C^{6+} at 100 MeV amu^{-1}. Our calculations have included a Fourier transformation from an impact parameter picture (in which the time-dependent calculations were performed) to a momentum transfer picture, which has allowed a quantitative comparison with the measurements of Schulz *et al* [1]. This current set of calculations is fully consistent with our earlier calculations [12], which presented angular distributions at specific impact parameters. We find that our calculations are generally in good agreement with measurement, and in particular we observe the double-peak structure in the perpendicular plane cross sections, which is also found experimentally. The calculated cross sections in this plane are smaller in magnitude than the measurements. However, this result is noteworthy as several previous sets of calculations have found a flat distribution in this plane.

It is difficult to pinpoint a single physical mechanism which is responsible for the double-peak perpendicular plane structures. However, for this feature to be found in a calculation, it appears necessary to provide an accurate treatment of the initial and final states of the system, as well as treating, in detail, the projectile–target interactions. Our calculations presented here treat all these aspects accurately. We note that somewhat similar conclusions may be drawn from a complementary study of fast electron-impact single ionization of He at 1 keV incident energy, where the 'perturbation' $|Z_P|/v_P$ is also close to 0.1 [18]. In that study, similar double-hump structures were found in the perpendicular plane measurements at similar kinematics (where in this case, the perpendicular plane was the plane perpendicular to the momentum transfer direction). A hybrid calculation, in which the projectile was described by a plane wave and the electron–target interactions described with an *R*-matrix with pseudo-states calculation, which also included the second-order interactions between the projectile and the target, was able to find similar double-hump structures in this plane. When the second-order interactions were omitted from the calculation, the angular distribution was almost flat in the perpendicular plane. We regard our findings described here as complementary to this previous electron-impact study [18]. Finally, we note that a recent study [19] suggests that the projectile coherence may have a much more important effect on the cross sections for ion impact than previously appreciated. In the study presented here, we treat the projectile classically, and so incoherently, as compared to previous plane-wave quantum-mechanical studies [3] which assumed a fully coherent projectile beam. This may provide a partial explanation for the previous discrepancies between theory and experiment for the differential cross sections under consideration here.

In the future, we plan further calculations in support of ion-impact single-ionization experiments, particularly for C^{6+} 2 MeV amu^{-1} impact, where the perturbation of the ion is much stronger. We also plan to extend our Fourier transform approach to double ionization, so that quantitative comparison may be made with future ion-impact double-ionization experiments which can measure fully differential cross sections.

Acknowledgments

We would like to thank Michael Schulz, Tom Kirchner and Don Madison for useful and enlightening discussions on many aspects of this work. The Los Alamos National Laboratory is operated by Los Alamos National Security, LLC, for the National Nuclear Security Administration of the US Department of Energy under contract no DE-AC5206NA25396. A portion of this work was performed through DOE and NSF grants to Auburn University. Computational work was carried out at NERSC, in Oakland, CA, and through a LANL Institutional Computing Resources award. MFC acknowledges the financial support of the MINCIN projects (FIS2008-00784 TOQATA and Consolider Ingenio 2010 QOIT).

References

[1] Schulz M, Moshammer R, Fischer D, Kollmus H, Madison D H, Jones S and Ullrich J 2003 *Nature* **422** 48
[2] Schulz M and Madison D H 2006 *Int. J. Mod. Phys.* A **21** 3649
[3] Madison D, Schulz M, Jones S, Foster M, Moshammer R and Ullrich J 2002 *J. Phys. B: At. Mol. Opt. Phys.* **35** 3297
[4] Voitkiv A B, Najjari B and Ullrich J 2003 *J. Phys. B: At. Mol. Opt. Phys.* **36** 2591
[5] Harris A L, Madison D H, Peacher J L, Foster M, Bartschat K and Saha H P 2007 *Phys. Rev.* A **75** 032718
[6] Fiol J, Otranto S and Olson R E 2006 *J. Phys. B: At. Mol. Opt. Phys.* **39** L285
[7] Dürr M, Najjari B, Schulz M, Dorn A, Moshammer R, Voitkiv A B and Ullrich J 2007 *Phys. Rev.* A **75** 062708
[8] Schulz M, Dürr M, Najjari B, Moshammer R and Ullrich J 2007 *Phys. Rev.* A **76** 032712
[9] Ciappina M F, Kirchner T and Schulz M 2010 *Comput. Phys. Commun.* **181** 813–20
[10] McGovern M, Assafrão D, Molhallem J R, Whelan C T and Walters H R J 2010 *Phys. Rev.* A **81** 042704
McGovern M, Whelan C T and Walters H R J 2010 *Phys. Rev.* A **82** 032702
[11] Pindzola M S, Robicheaux F and Colgan J 2007 *J. Phys. B: At. Mol. Opt. Phys.* **40** 1695
[12] Pindzola M S, Robicheaux F and Colgan J 2010 *Phys. Rev.* A **82** 042719
[13] Bransden B H and McDowell M R C 1992 *Charge Exchange and the Theory of Ion–Atom Collisions* (Oxford: Clarendon)
[14] Gulyás L, Igarashi A, Fainstein P D and Kirchner T 2008 *J. Phys. B: At. Mol. Opt. Phys.* **41** 025202
[15] Járai-Szabó F and Nagy L 2007 *J. Phys. B: At. Mol. Opt. Phys.* **40** 4259
[16] Foster M, Colgan J and Pindzola M S 2008 *Phys. Rev. Lett.* **100** 033201
[17] Arfken G B and Weber H J 2001 *Mathematical Methods for Physicists* (San Diego, CA: Harcourt/Academic Press)
[18] Dürr M, Dimopoulou C, Najjari B, Dorn A, Bartschat K, Bray I, Fursa D V, Chen Z, Madison D H and Ullrich J 2008 *Phys. Rev.* A **77** 032717
[19] Egodapitiya K N, Sharma S, Hasan A, Laforge A C, Madison D H, Moshammer R and Schulz M 2011 *Phys. Rev. Lett.* **106** 153202